Received: 23 June 2023 | Revised: 14 December 2023 | Accepted: 11 January 2024

DOI: 10.1111/psyp.14529

PSYCHOPHYSIOLOGY SPR WILEY

ORIGINAL ARTICLE

Mapping the routes of perception: Hemispheric asymmetries in signal propagation dynamics

Davide Bonfanti | **Chiara Mazzi** | **Silvia Savazzi**

Perception and Awareness (PandA) Laboratory, Department of Neuroscience, Biomedicine and Movement Sciences, University of Verona, Verona, Italy

Correspondence
Chiara Mazzi, Perception and Awareness (PandA) Laboratory, Department of Neuroscience, Biomedicine and Movement Sciences, University of Verona, Verona, Italy.
Email: chiara.mazzi@univr.it

Funding information
CARIVERONA FOUNDATION, Grant/Award Number: 2018.0861; Ministero dell'Istruzione, dell'Università e della Ricerca, Grant/Award Number: 2017TBA4KS_002 and 737/2021; MNESYS, Grant/Award Number: DN. 1553 11.10.2022

Abstract

The visual system has long been considered equivalent across hemispheres. However, an increasing amount of data shows that functional differences may exist in this regard. We therefore tried to characterize the emergence of visual perception and the spatiotemporal dynamics resulting from the stimulation of visual cortices in order to detect possible interhemispheric asymmetries. Eighteen participants were tested. Each of them received 360 transcranial magnetic stimulation (TMS) pulses at phosphene threshold intensity over left and right early visual areas while electroencephalography was being recorded. After each single pulse, participants had to report the presence or absence of a phosphene. Local mean field power analysis of TMS-evoked potentials showed an effect of both site (left vs. right TMS) of stimulation and hemisphere (ipsilateral vs. contralateral to the TMS): while right TMS determined early stronger activations, left TMS determined later stronger activity in contralateral electrodes. The interhemispheric signal propagation index revealed differences in how TMS-evoked activity spreads: left TMS-induced activity diffused contralaterally more than right stimulation. With regard to phosphenes perception, distinct electrophysiological patterns were found to reflect similar perceptual experiences: left TMS-evoked phosphenes are associated with early occipito-parietal and frontal activity followed by late central activity; right TMS-evoked phosphenes determine only late, fronto-central, and parietal activations. Our results show that left and right occipital TMS elicits differential electrophysiological patterns in the brain, both per se and as a function of phosphene perception. These distinct activation patterns may suggest a different role of the two hemispheres in processing visual information and giving rise to perception.

KEYWORDS
early visual cortex, hemispheric asymmetries, interhemispheric differences, phosphenes, TMS-EEG, visual awareness

Abbreviations: EEG, electroencephalography; GMFP, global mean field power; ICA, independent component analysis; ISP, interhemispheric signal propagation; LMFP, local mean field power; MSO, maximum stimulator output; TEP, TMS-evoked potential; TMS, transcranial magnetic stimulation.

1 | INTRODUCTION

In the last few decades, a series of studies has started to investigate possible differences in visual processing between the left and right hemispheres. A hemispheric equivalence has often been assumed, given the low level of the involved functions; however, a wealth of results points now to the fact that the two hemispheres are responsible for processing different characteristics of visual stimuli (Fink et al., 1996, 1997; Hellige, 1996; Lux et al., 2004; Robertson et al., 1988): while the right is specialized in providing coarse, structural information, the left contributes to analyzing fine-grained visual details about the stimulus.

Robertson et al. (1988) reported that lesions to right temporo-parietal regions affected the processing of the global level of hierarchical stimuli (i.e., Navon letters), while damage to the left superior temporal gyrus impaired local components analysis. Differences in the processing of local and global aspects of stimuli were also reported in healthy participants: in a series of fMRI studies, Fink et al. (1996, 1997) reported that the right lingual gyrus is responsible for global-level analysis of Navon letters, while the left inferior occipital cortex oversees local elements processing. Further strong confirmation of this asymmetry comes from a work of Lux et al. (2004) reporting that, when a global stimulus is displayed in the right visual hemifield, there is increased neural activity in the right posterior occipital cortex. On the contrary, when a local stimulus is shown within the left hemifield, the left posterior occipital cortex is activated. This shows that stimulus information can traverse the corpus callosum to reach the hemisphere specialized for either local or global processing.

Recently, these two different levels of visual processing have been linked with low and high spatial frequencies (LSF, HSF), which have been identified as the visual characteristics responsible for global and local representation, respectively (Peyrin et al., 2003, 2004, 2005). Numerous papers (Kitterle et al., 1990; Peyrin et al., 2006; Proverbio et al., 1996) have shown the existence of a hemispheric asymmetry recalling the one for global and local processing (Sergent, 1982). For example, in an fMRI study by Musel et al. (2013) a right occipito-temporal predominance was found for LSF image processing during a categorization task, while a left temporal predominance was found for HSF stimuli. Another fMRI experiment aiming at comparing the spatial frequency bands in the two hemispheres (Peyrin et al., 2004) has shown that within the early visual areas, there is a right-hemispheric predominance for LSF processing and a left predominance for HSF processing.

Other works have suggested the existence of hemispheric differences after the presentation of visual stimuli. For example, Chokron et al. (2016) have outlined how the exact nature of the visual deficit in hemianopic patients is influenced by the lesion side, with performance in different tasks impaired according to the lesion being located in the right or left occipital cortex. In an EEG study, Sanchez-Lopez et al. (2020) reported that showing a stimulus after either a valid or invalid cue elicited a differential time-frequency activity depending on the hemifield of presentation.

Taken together, these results point toward asymmetric hemispheric processing of visual information, with the right hemisphere more involved in coarse visual analysis and the left hemisphere handling finer details. However, most of these studies rely on imaging techniques, like EEG and fMRI, which are bound to establish correlational relationships. Therefore, we tried to fill this gap by directly probing lateralized differences in the visual system by stimulating the early visual areas of the two hemispheres with single-pulse TMS, while recording the elicited activity with EEG. TMS is known for eliciting phosphenes (i.e. experiences of flashes of light in the absence of any external stimulus) when targeted over early visual areas (Bagattini et al., 2015). Indeed, the combined use of these two techniques consents to noninvasively stimulate selected cortical regions and track the corresponding spatiotemporal activity (Rosanova et al., 2012); the recorded activations are therefore directly caused by the TMS pulse. Therefore, eliciting phosphenes from both hemispheres allows to assess the potential differences between the two hemispheres in generating visual percepts, shedding more light on possible hemispheric differentiations in perceptual spatiotemporal dynamics. An asymmetry in the electrophysiological activations related to phosphene presence would strongly suggest that the two hemispheres exhibit lateralized differences in their spatiotemporal dynamics during visual perception. A better comprehension of the hemispheric dynamics associated with visual perception may pave the way for improved treatments able to restore visual functions in patients suffering from cortical blindness (Meikle & Wong, 2022).

2 | MATERIALS AND METHODS

2.1 | Participants

Twenty-two volunteers (9 males, mean age 24.09 ± 4.05) with normal or corrected-to-normal vision participated in the study and were reimbursed for their participation. Data from four participants were excluded from the analyses because of either technical issues or excessively long reaction times (RTs). Written informed consent was obtained according to the 2013 Declaration of Helsinki.

The experimental protocol has been approved by the local Ethics Committee.

Participants were screened by a safety questionnaire (adapted from (Rossi et al., 2009)) for the risk factors associated with TMS and none reported any contraindications.

Handedness was assessed by means of the Edinburg inventory (Oldfield, 1971). All recruited participants showed a high tendency for right-handedness (mean 85.77) with very low internal variability (SEM 2.99).

2.2 | MRI image acquisition

Each participant underwent MRI with a 1.5 Tesla Philips scanner. We acquired a whole-brain high-resolution 3D T1-weighted image with magnetization-prepared rapid acquisition gradient echo (TR 7.7 ms/TE 3.5).

2.3 | TMS protocol

We delivered single-pulse TMS via a 70 mm figure-of-eight coil connected with a Magstim Rapid2 system (maximum output 3.5 T, Magstim Company Limited, Whitland, UK). We placed the TMS coil tangentially to the surface of the scalp, with the handle pointing upward to avoid unspecific activation of neck muscles.

Stimulation sites corresponding to left and right early visual areas were functionally located through phosphene induction. The electrode positions O1 (left hemisphere) and O2 (right hemisphere) of the 10–20 EEG system (Mazzi et al., 2014) were used as a starting reference around which (~2 cm^2 area, centered on the target electrodes) the hotspot eliciting the clearest and most consistent phosphenes at supra-threshold intensity was selected. Neuronavigation based on individual MRI images (SofTaxic, E.M.S., Bologna, Italy and Polaris Vicra, NDI, Waterloo, Canada) was used (1) in the course of the hotspot search to constantly check that the focus of stimulation belonged to early visual areas, (2) during the experiment to monitor for possible coil displacements within a 2 mm accuracy threshold, and (3) to accurately reposition the coil over the hotspot after participants' break.

To determine the individual phosphene threshold (PT) for the two stimulation sites, we employed the automatic procedure of the "method of constant stimuli" (MOCS) (Mazzi, Savazzi, et al., 2017). First, the hotspot was functionally identified for each of the two stimulation sites, and afterwards the PT was assessed by means of a computerized MOCS version: seven TMS intensities were randomly used (ranging from 60% to 78% of MSO, with increases in steps of 3%). Seven pulses were delivered for each intensity, for a total of 49 pulses, and for each of them, participants had to report the eventual phosphene presence. Data were fitted with a cumulative logistic psychometric function via a maximum likelihood criterion using the Matlab Palamedes toolbox (http://www.palamedestoolbox.org). From the resulting function, the intensity at which participants perceived phosphenes in 50% of trials was taken as the PT and used as stimulation intensity in the experimental phase.

2.4 | Experimental procedure

Participants were tested in a dark room. They sat in front of a monitor with their head secured in a chin rest to keep their eyes aligned with the central fixation point, where participants were instructed to maintain their fixation throughout the experiment.

Before the experiment, participants were tested for the perception of genuine phosphenes in a training session (Figure 1a). They were initially debriefed about TMS functioning and phosphenes (Kammer et al., 2005; Mazzi, Savazzi, et al., 2017). Participants wore a cap on which the positions of O1 and O2 electrodes were highlighted. They seated in a dark room in front of a black screen showing a fixation point. Experimenters started administering single-pulse TMS around O1/O2 position, asking after each pulse if the participant had seen something in their visual field that matched the phosphenes characteristics, and, if so, to give a short description of it in terms of position, shape, color, and texture. Once the experimenters were confident that participants had sufficiently adapted to darkness and that they were perceiving actual phosphenes, they started changing stimulation conditions (e.g. asking them to close their eyes to fixate on a different point on the screen) to see if participants' answers matched the expected characteristics for phosphenes. Once the perception of phosphenes for one hemisphere was ascertained, the same procedure was repeated for the other hemisphere.

The criteria used to test for a genuine phosphene are described in Kammer et al. (2005): according to the authors, phosphenes appear in the visual field contralateral to the stimulated hemisphere, following the contralateral organization of the brain; they must follow the participant's gaze, that is, if they fixate a different point, phosphenes should follow the eye movement; they should appear independently of the eyes being open or closed.

After having been tested for genuine phosphenes perception, participants underwent an MRI scan necessary for neuronavigated TMS.

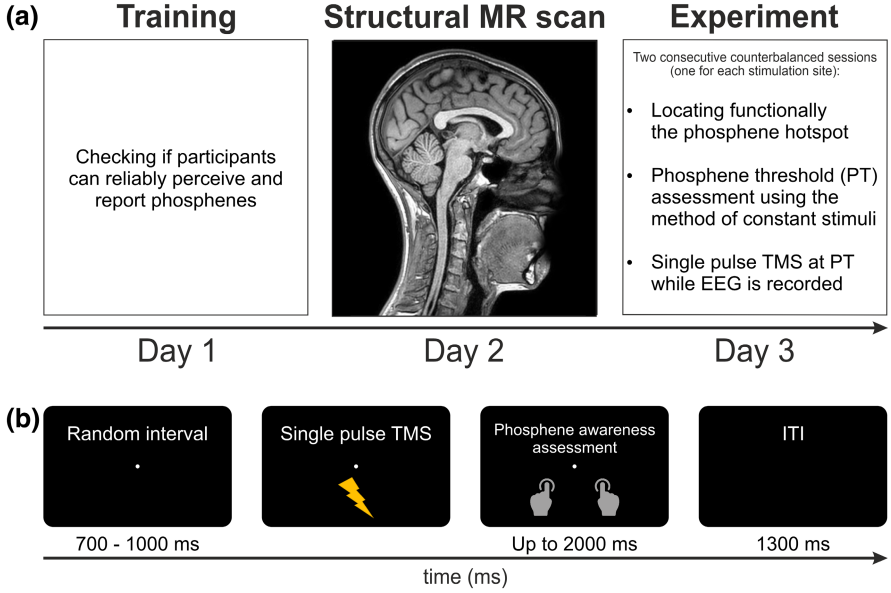

FIGURE 1 Experimental procedure and trial structure. (a) Outline of the experimental procedure for each participant. (b) Outline and timing of each stimulation trial.

During the experimental sessions, single-pulse TMS to the left or right occipital cortex was administered at PT intensity while recording EEG. In order to mask the TMS click, participants were asked to wear disposable earplugs. The order of the two stimulation sites was counterbalanced across participants. Each trial started with a random interval comprised between 700 and 1000 ms, followed by a TMS pulse. Regardless of the stimulation side, participants had up to 2000 ms after each pulse to report the presence of a phosphene by pressing on the keyboard the "m" key with their right hand or to report the absence of a phosphenes by pressing the "z" key with their left hand, followed by 1300 ms of intertrial interval (Figure 1b). They underwent two consecutive sessions—one for each stimulation site—of 360 pulses each, divided into 6 blocks of 60 trials to prevent excessive fatiguing. Between one block and the other, participants could rest for a few minutes, and the experimenters entered the room to check in on participants.

2.5 | EEG recording and preprocessing

We used TMS-compatible EEG equipment (BrainAmp, Brain Products GmbH, Munich, Germany) to register EEG activity (BrainVision Recorder), combined with a Fast'n East cap with 59 TMS-compatible Ag/AgCl pellet pin electrodes (EasyCap GmbH, Herrsching, Germany) placed following the extended 10–20 International System. Additional electrodes were used as online reference (RM), ground (AFz) and to monitor horizontal and vertical eye movements. Electrode impedance was kept below 5 KΩ.

To reduce TMS-related artifacts and enable EEG recording from the electrodes underneath the TMS coil, a custom-made polystyrene C-shaped annulus was positioned over the target electrode (Bagattini et al., 2015).

We processed the EEG signal off-line using Matlab 2021b (Mathworks, USA) with the EEGLAB toolbox (version 2021.0, (Delorme & Makeig, 2004)) and the TMS-EEG signal analyzer (TESA) extension (Rogasch et al., 2017).

First, the continuous raw signal digitized at 5000 Hz was segmented 1000 ms before and after the TMS pulse. Epoched data were demeaned using the whole epoch, and the TMS pulse artifact was removed from −2 to 10 ms. We then replaced it with cubic interpolation to avoid ringing artifacts. Data were then downsampled at 500 Hz. A first round of independent component analysis (ICA) (Delorme et al., 2007) was performed for each participant to remove the tail-end of the remaining muscle artifact induced by TMS (Rogasch et al., 2017). In this round of ICA, an average of 0.44 ± 0.51 components was removed from O1 data sets, and an average of 0.5 ± 0.7 components was removed from O2 data sets. No significant differences in the number of removed components were detected between the two conditions [$t(1,17) = -0.566$; $p = .579$, Cohen's $d = -0.133$]. Data were then bandpass filtered (0.1–100 Hz, zero-phase, fourth-order Butterworth bandpass) and band-stop filtered (49–51 Hz). A second run of ICA screened for blinks, lateral eye movements, persistent muscle activity, and electrode noise. In this second round of ICA, an average of 28.16 ± 7 components was removed from O1 data sets, and an average of 28.66 ± 5.34 components was removed from O2 data sets. No significant differences in the number of removed components were detected between the two conditions [$t(1,17) = -0.423$; $p = .678$, Cohen's $d = -0.100$]. To improve component decomposition, interpolated data from −2 before to 10 ms after TMS pulse were substituted with constant amplitude values before each ICA and interpolated again thereafter. Data were then re-referenced to a point at infinity (Yao, 2001) through the REST toolbox (Dong et al., 2017), low-pass filtered at 40 Hz, and

epoched from −100 to 500 ms. We then flipped O2 data sets, so that the stimulation sites were overlapped in the two experimental sessions. Data sets were then appended and downsampled at 250 Hz; bad trials were automatically detected and rejected through the EEGLAB's TBT toolbox (Ben-Shachar, 2020) (extreme values thresholds: ±125 μV, improbability and kurtosis criteria for single channels: SD > 5, for global threshold: SD > 3, maximum slope allowed: 50 μV, and minimal R^2 allowed: 0.3). We finally performed baseline correction from −100 to 0 ms.

To better characterize the TMS-evoked activity as a function of the hemisphere, for each participant we computed the LMFP (Lehmann & Skrandies, 1980) as the square root of the squared TEPs across the electrodes located on each of the two hemispheres (i.e. we considered all left or right electrodes to calculate a "hemispheric" LMFP, so that ipsilateral and contralateral electrodes with respect to the stimulation site were taken into account separately; midline electrodes were excluded from this analysis).

For the two stimulation sites, we also computed a modified version of the ISP index, a measure already used in literature to evaluate interhemispheric cortico-cortical dynamics (Casula et al., 2020; Hui et al., 2021; Jarczok et al., 2016; Voineskos et al., 2010). For each participant, we calculated the ISP index for each pair of homologue scalp electrodes (excluding vertical midline) following this formula:

$$\text{ISP} = \text{rectified}\,(\text{TMS} - \text{evoked activity contralateral} / \text{TMS} - \text{evoked activity ipsilateral})$$

We obtained thus 26 ISP values per participant (ISP values exceeding 3.5 standard deviations were classified as outliers and not included in the following steps), differently from previous authors which calculated the ISP index only on the stimulated electrode or on a limited cluster of surrounding electrodes. Notably, the obtained values were then averaged in order to get a single value for each participant, therefore providing an overview of the interhemispheric dynamics of the whole scalp. We refer to this single value as global ISP (gISP). This procedure was repeated across five subsequent time windows identified around the peaks of the LMFP: 12–24, 24–48, 48–92, 92–124, and 124–240 ms. For the electrodes contralateral to the stimulation site, the latency of the time windows was shifted by 4 ms, accounting for interhemispheric transfer time (Marzi et al., 1991).

2.6 | Behavioral statistics

Behavioral data were analyzed with JASP (JASP Team, 2020). First, PT values of the two stimulation sites were compared using a paired samples *t*test. Then, a cut-off procedure was applied to exclude trials from the experimental sessions with RTs < 150 ms or >3 SD. A one-sample *t* test was performed to check if the percentages of detected phosphenes differed from 50%. A 2×2 ANOVA with *stimulation site* (O1|O2) and *phosphene awareness* (present|absent) as within-subjects factors was carried out on RTs.

2.7 | LMFP statistics

LMFPs were compared via a series of 2×2 ANOVAs with *stimulation site* (O1|O2) and *hemisphere* (ipsilateral|contralateral to the stimulation) as within-subject factors for each time point.

2.8 | gISP statistics

A 2×5 ANOVA was performed on gISP values, with *stimulation site* (O1|O2) and *time window* (12–24 ms|24–48 ms|48–92 ms|92–124 ms|124–240 ms) as factors, with multiple paired *t* tests used as post hoc analysis to check for possible effects on the interaction. A Greenhouse–Geisser correction was used for sphericity, and false discovery rate (FDR) (Groppe et al., 2011) was used to control for multiple comparisons when applicable.

2.9 | TEPs statistics

With the aim of giving a full characterization of TEP responses across all the electrodes and the entire epoch, we used the LIMO toolbox for EEGLAB (Pernet et al., 2011) to perform 2×2 ANOVAs with *stimulation site* (O1|O2) and *phosphene awareness* (present|absent) as within-subject factors, followed by *t* tests to disentangle the interaction between factors. These results were then temporally thresholded using temporal clustering so that only significant activations equal to or longer than 12 ms were considered.

3 | RESULTS

3.1 | Behavioral results

Figure 2a shows stimulation sites for each participant. The mean PT was reached for the left stimulation site at 69% of MSO and at 68.8% of MSO for the right stimulation site (Figure 2b). These two values were not significantly different [$t(17) = 0.450$; $p = .658$].

We also checked if the mean percentage of phosphenes detected through the experiment was significantly different from 50%: this is not the case for both stimulation sites

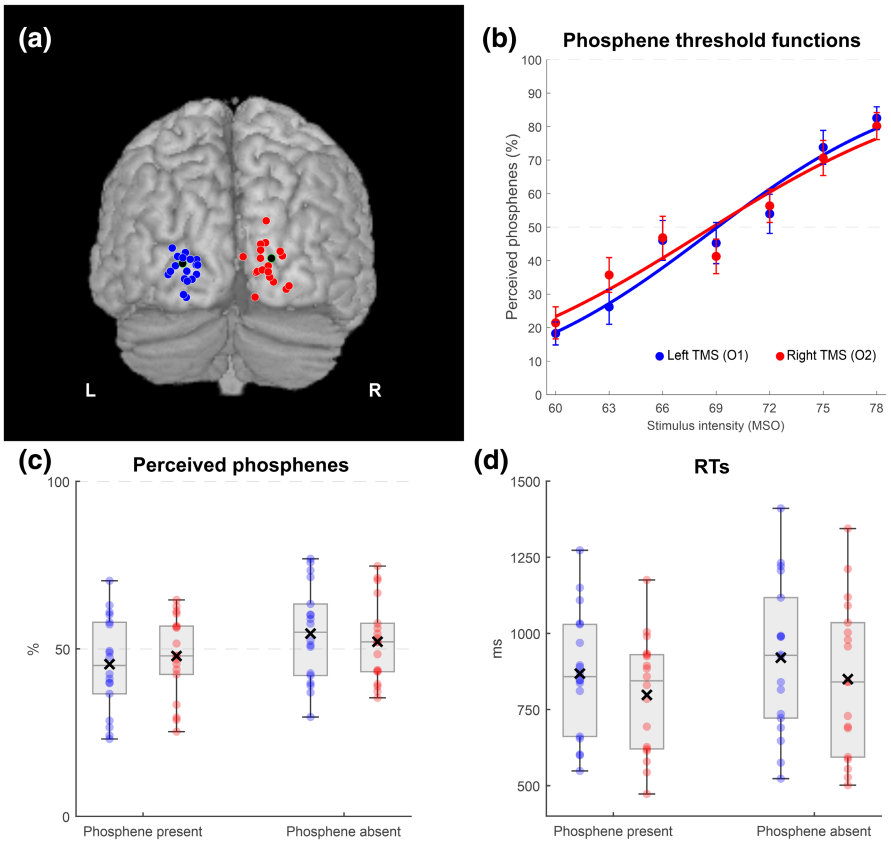

FIGURE 2 Stimulation sites, phosphene threshold functions, and behavioral results. (a) Stimulation sites for each participant in the two hemispheres. Each dot corresponds to an individual hotspot eliciting phosphenes. Red dots represent left TMS, blue dots represent right TMS. Black dots respectively correspond to the O1 and O2 electrode positions. (b) Average phosphene threshold functions for right and left occipital TMS. The intensity at which participants reported a phosphene on 50% of pulses was selected as the stimulation intensity for the experimental sessions. Each dot represents the average number of phosphenes reported for that specific stimulation intensity; the fitted functions illustrate the average phosphene threshold functions across participants. Error bars represent standard errors of the mean (SEM). (c) Percentages of reported phosphenes for the two stimulated sites. (d) Reaction times for phosphene present and absent trials for the two stimulated sites. Colored dots represent individual data.

[O1: $t(17) = -1.354$; $p = .194$; O2: $t(17) = -0.737$; $p = .471$], thus supporting our procedure for establishing PT and an equal distribution of trials between conditions. On average, participants reported a phosphene in the 45.4% of trials when stimulated over O1, and in the 47.8% of trials when stimulated over O2 (Figure 2c).

The ANOVA on RTs detected a significant main effect of *stimulation site* [$F(1,17) = 5.520$; $p < .05$; $\eta_p^2 = 0.245$] and *phosphene awareness* [$F(1,17) = 5.122$; $p < .05$; $\eta_p^2 = 0.232$] with RTs overall faster following phosphene perception and O2 stimulation, respectively. No interaction occurred between the two factors [$F(1,17) = 1.985e{-4}$; $p = .989$; $\eta_p^2 = 1.167e{-5}$] (Figure 2d).

3.2 | LMFP results

A series of 2×2 ANOVAs with *stimulation site* (O1|O2) and *hemisphere* (ipsilateral|contralateral to the stimulation) as factors was performed over LMFP data, which were calculated by pooling over, respectively, the electrodes ipsilateral and contralateral to the stimulation. This analysis revealed a significant effect of the stimulation site in the time range between 16 and 28 ms [all $ps < .05$]. Considering the hemisphere, we found significant differences between ipsi- and contralateral hemispheres to the stimulation site in the time range between 20 and 48, 56 and 64, and 108 and 120 ms [all $ps < .05$]. The interaction between the factors was significant in the time range between 76 and 84 ms: post-hoc *t* tests revealed a significant difference between the LMFP of the two hemispheres contralateral to the stimulation in the time range between 80 and 84 ms [all $ps < .05$] (Figure 3a), with LMFP from the hemisphere contralateral to left TMS (i.e. right hemisphere) being higher than LMFP from the hemisphere contralateral to right TMS (i.e. left hemisphere).

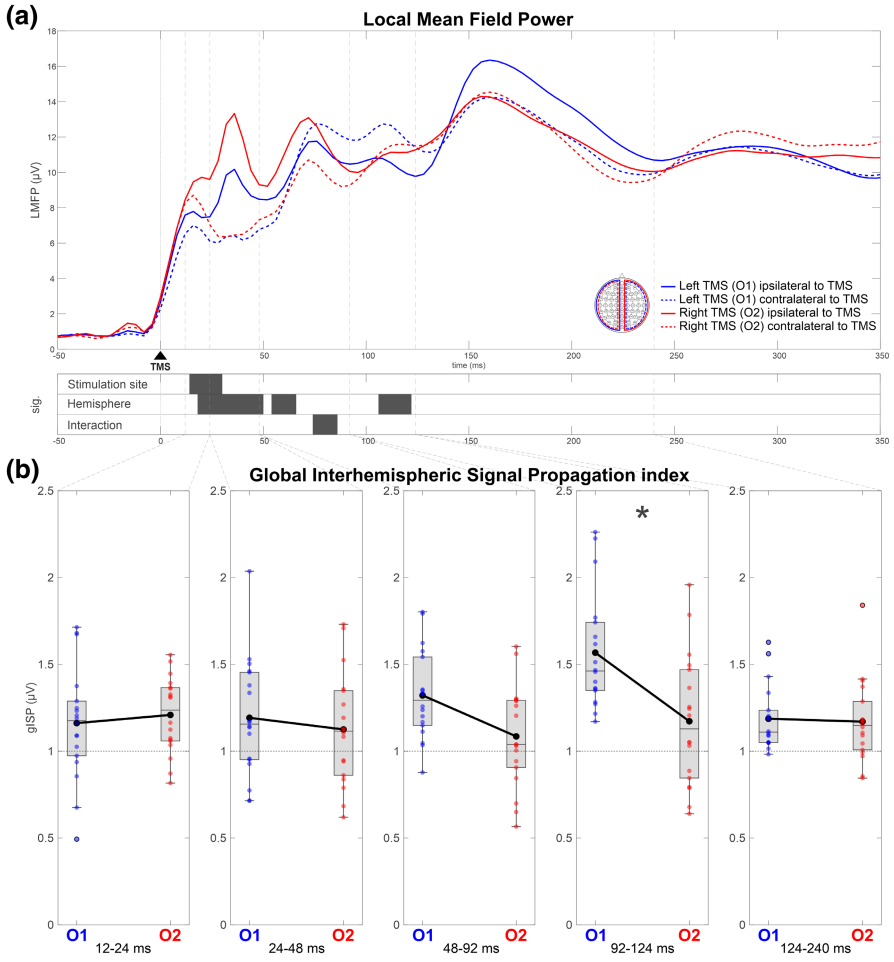

FIGURE 3 LMFP and gISP results. (a) LMFP calculated separately for the electrodes ipsilateral and contralateral to the stimulation (vertical midline electrodes were not considered), for each stimulation site. Gray bars below the plot highlight significant results for each factor (stimulation site, hemisphere, and the interaction between the two). (b) gISP results (obtained by averaging the ISP values calculated for each pair of homologue electrodes and excluding vertical midline electrodes) for the five time windows selected around the peaks of LMFP. The two vertical axes of each plot represent, respectively, the gISP values corresponding to O1 (in blue) and O2 (in red) stimulation. The thick black line corresponds to the averaged gISP value across electrode pairs and participants. Colored dots represent individual data.

3.3 | gISP results

On the gISP data (calculated over every couple of homologue scalp electrodes), we performed a 2×5 ANOVA with *stimulation site* (O1|O2) and *time window* (12–24 ms|24–48 ms|48–92 ms|92–124 ms|124–240 ms) as factors. This analysis revealed a significant main effect of stimulation site [$F(1,17)=4.768$; $p<.05$, $\eta_p^2=0.219$] and time window [$F(2.606,44.302)=3.892$; $p<.05$, $\eta_p^2=0.186$]; also the interaction was found to be significant [$F(2.816,47.876)=3.889$; $p<.05$, $\eta_p^2=0.186$] (Figure 3b).

To disentangle the significant interaction, we performed a series of *t* tests, which revealed that in the fourth time window (92–124 ms) left TMS elicited a higher gISP compared to right TMS [$t(17)=2.9420$; $p=.0456$, Cohen's $d=0.693$], while in the other time windows there was no differences between the two stimulation sites (W1 [$t(17)=-0.4783$; $p=.7851$], W2 [$t(17)=0.7851$; $p=.5257$], W3 [$t(17)=2.3717$; $p=.0745$], and W5 [$t(17)=0.2770$; $p=.7851$]) meaning that left TMS elicited a higher amplitude in contralateral electrodes than in ipsilateral ones compared to right TMS.

3.4 | TEPs results

A 2×2 repeated measure ANOVA with *stimulation site* (O1|O2) and *phosphene awareness* (present|absent) was carried out as within-subject factors.

To report significant TEP results, temporal clusters around GMFP peaks were identified. A complete overview of the significant time windows of all electrodes for each statistical comparison can be found in Table 1.

3.4.1 | Stimulation site

The two-way repeated measure ANOVA carried out on TEPs (Figure 4a) revealed a significant effect [all $ps<.05$] of *stimulation site*. Three main clusters were highlighted: the first one in the 92–128 ms time window developed mainly over right fronto-central electrodes; the second one in the 128–236 ms time window involved right frontal and left parietal electrodes; and the last one in the 236–348 ms time window was present on fronto-parietal electrodes (Figure 4b).

TABLE 1 Summary of the significant TEPs results. Each column represents a statistical comparison, and each row represents a different electrode. The milliseconds reported in each slot represent the time windows in which a certain statistical comparison is significant at that specific electrode.

	Stimulation site	Phosphene awareness	Interaction	Left TMS (O1)	Right TMS (O2)
O1				64–84; 164–204	216–244
Oz		72–84; 164–176	172–188	68–84; 164–200	
O2		152–176	176–196	172–196	
PO7	152–168	68–80		64–80; 168–204	216–236
PO3		68–80; 304–324		68–80; 172–200	
POz		304–324			300–324
PO4					296–324
PO8		144–168; 196–224	180–200	76–88	104–116
P7	156–204; 324–348				200–260; 296–336
P5	160–188; 220–348	64–80		68–84; 168–200	188–256
P3		68–80; 300–328		68–80	
P1		280–348			
Pz		236–264; 272–348		240–256	284–348
P2		308–320; 336–348		232–260	208–220; 280–348
P4					288–348
P6		152–168; 188–228	184–196		292–320
P8		140–164; 188–224	180–196	152–164	
TP7	168–204			276–296; 312–340	188–348
CP5			212–224	64–80; 168–180; 264–292; 328–340	172–332
CP3		296–348	64–80	64–84	212–224
CP1		132–160; 208–348		308–324	296–316; 332–348
CPz	88–124	132–348		136–156; 228–348	132–144; 160–224; 232–348
CP2		232–348		140–152; 228–348	132–348
CP4	108–128			272–288; 312–348	204–220; 272–348
CP6	104–132	132–152; 180–228; 256–280	88–100; 124–148	88–100; 116–140	288–336
TP8	232–328	132–156; 196–228; 248–348	120–152	124–152	
T7	108–124			248–296; 312–348	192–348
C5	112–136		212–224; 304–316	68–80; 168–180; 252–292; 320–348	168–348
C3		136–156; 252–348			180–228; 248–280
C1		124–212; 220–348	260–272	140–156; 252–264; 276–296; 312–324	132–160
Cz	100–120	124–348		132–164; 228–348	124–348
C2	84–128	136–168; 236–264; 272–348		144–160; 232–348	124–348
C4	92–132		32–44; 116–152; 196–216	92–120; 280–292; 308–348	140–176; 192–348
C6	108–128; 232–292	116–152; 184–232; 248–292; 308–320	112–156	96–144	144–156; 196–208; 304–328
T8	240–288	136–148; 212–236; 244–348	120–152; 252–276		
FT7	104–144		176–220	240–256; 268–288; 316–348	176–348
FC5	120–144		180–204	320–348	176–348

TABLE 1 (Continued)

	Stimulation site	Phosphene awareness	Interaction	Left TMS (O1)	Right TMS (O2)
FC3		140–156; 280–340	252–272		
FC1		136–172; 248–348	256–272	144–156; 284–296	
FCz	100–124	124–180; 236–348		132–184; 236–336	136–168; 304–348
FC2	72–136	140–156; 296–348		236–348	252–264; 296–348
FC4	76–144			280–348	140–152; 228–240; 248–348
FC6	88–132	204–320		68–80	312–332
FT8		228–348	244–288		192–204
F7				316–348	176–236; 280–348
F5	324–348			332–348	176–332
F3			180–200; 256–272		
F1		304–348	92–104; 180–200; 252–280	256–272	
Fz	108–120		12–28; 92–108; 180–200; 256–280	140–156; 168–200; 240–300	
F2	80–128		12–28; 96–108	172–196; 240–308; 320–340	320–348
F4	88–124		12–24; 96–108	56–80; 172–200; 244–308; 320–348	316–348
F6	160–172; 320–348	120–144	12–24	60–80; 328–348	252–264
F8	160–176; 224–348	128–148; 280–324	228–240; 252–272	64–80	220–232; 252–264
AF7					120–132; 284–348
AF3			88–104; 184–196		
AF4	152–172; 336–348		12–28; 68–80; 88–108	52–80; 168–204; 244–288	
AF8	152–184; 220–348	124–136		64–84; 188–204; 332–348	196–232; 244–288
FP1					
FP2	332–348		72–84; 92–104	60–84; 168–204; 252–272	

3.4.2 | Phosphene awareness

The two-way repeated measure ANOVA carried out on TEPs (Figure 5a) revealed a significant effect [all *p*s < .05] of *phosphene awareness*. Three clusters could be highlighted: the first one in the 48–92 ms time window comprised left parieto-occipital electrodes; the second one in the 124–240 ms time window involved mainly right fronto-central and parietal electrodes; and the third one in the 240–348 ms time window developed mainly over right fronto-central and bilateral parietal electrodes (Figure 5b).

3.4.3 | Stimulation site by phosphene awareness interaction

Looking at the interaction, we identified four different clusters: the first one in the 12–24 ms time window involving right frontal and left temporal electrodes; the second one in the 96–128 ms time window comprising right frontal and central electrodes; the third one in the 128–240 ms time window including bilateral fronto-central and parieto-occipital electrodes; the fourth cluster (240–316 ms time window) comprising bilateral fronto-temporal electrodes (Figure 6).

To disentangle the contribution of the different factors in the interaction, we looked at *t* tests showing the different awareness-related activity in the two stimulation sites. When contrasting TEPs of phosphene present versus phosphene absent trials following O1 stimulation (Figure 7a), we identified four different clusters: the first one in the 56–96 ms time window comprised left occipito-temporal and right frontal electrodes; the second one in the 96–128 ms time window comprised central electrodes; the third one in the 128–240 ms time window comprised mainly right fronto-central and bilateral parieto-occipital electrodes, while the last cluster (240–348 ms time window) comprised bilateral fronto-central and centro-parietal electrodes (Figure 7b).

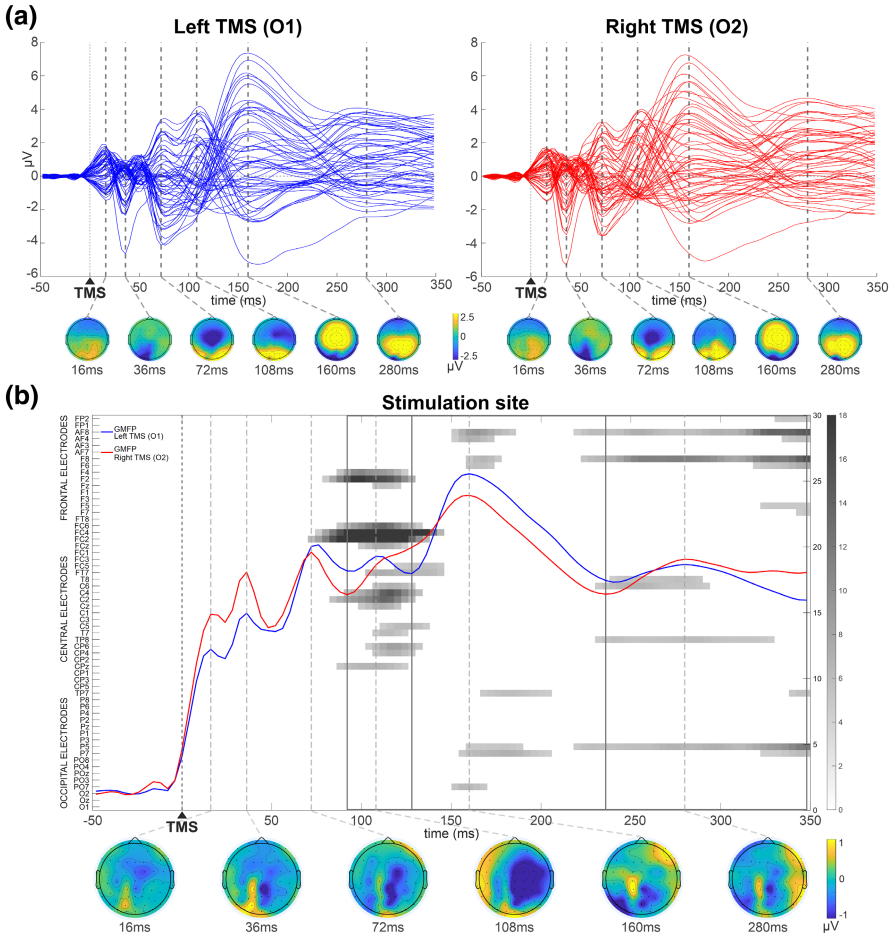

FIGURE 4 Results from the ANOVA conducted on TEPs: main effects of "stimulation site." (a) Butterfly plots depicting TEPs for the two *stimulation site* conditions ("Left TMS over O1", blue; "Right TMS over O2", red). Vertical dotted lines highlight the peaks of the different TEPs components. The scalp topographies below represent the scalp topographic distribution for each component peak. (b) Raster plot depicting for each time point and each electrode the significant differences (expressed in *F*-values) between "Left TMS" and "Right TMS." Right TMS data were flipped so that stimulation sites were overlapped. *X* and *Y* axis represent, respectively, time in milliseconds and electrodes (from posterior to anterior ones). The two lines superimposed represent the GMFPs associated with the two *Stimulation site* conditions, whose peaks were used to identify TEPs clusters. The vertical dotted lines highlight GMFPs peaks. The scalp topographies below represent scalp differences between the two conditions ("Left TMS"–"Right TMS"), with each map corresponding to the latency of each GMFP peak.

When contrasting TEPs of phosphene present versus phosphene absent trials following O2 stimulation (Figure 8a), two clusters emerged: the first one in the 128–236 ms time window comprised bilateral frontocentral and parieto-occipital electrodes; the second one in the 236–348 ms time window comprised bilateral frontocentral and parietal electrodes (Figure 8b).

4 | DISCUSSION

In this TMS-EEG study, we aimed at confronting the spatiotemporal dynamics associated with visual perception between the two hemispheres. To do so, we stimulated with TMS at threshold intensity the left and right early visual cortex to elicit phosphenes, that is, conscious visual percepts known to be processed similarly to real external stimuli (Knight et al., 2015a, 2015b; Mazzi et al., 2014), while simultaneously recording EEG activity. The comparison of LMFPs across the two stimulation sites showed that TMS elicits different patterns of electrophysiological activity as a function of the stimulation site and the hemisphere: while right occipital TMS determined early stronger activations, left occipital TMS elicited late higher activity circumscribed to electrodes contralateral to the stimulation site.

The temporal dynamics of LMFP are mirrored by the differences in RTs between the two stimulated sites, with responses after right TMS being significantly faster than left-sided responses. This suggests a faster processing by the right hemisphere after occipital stimulation than by the left hemisphere, hinting at the existence of a

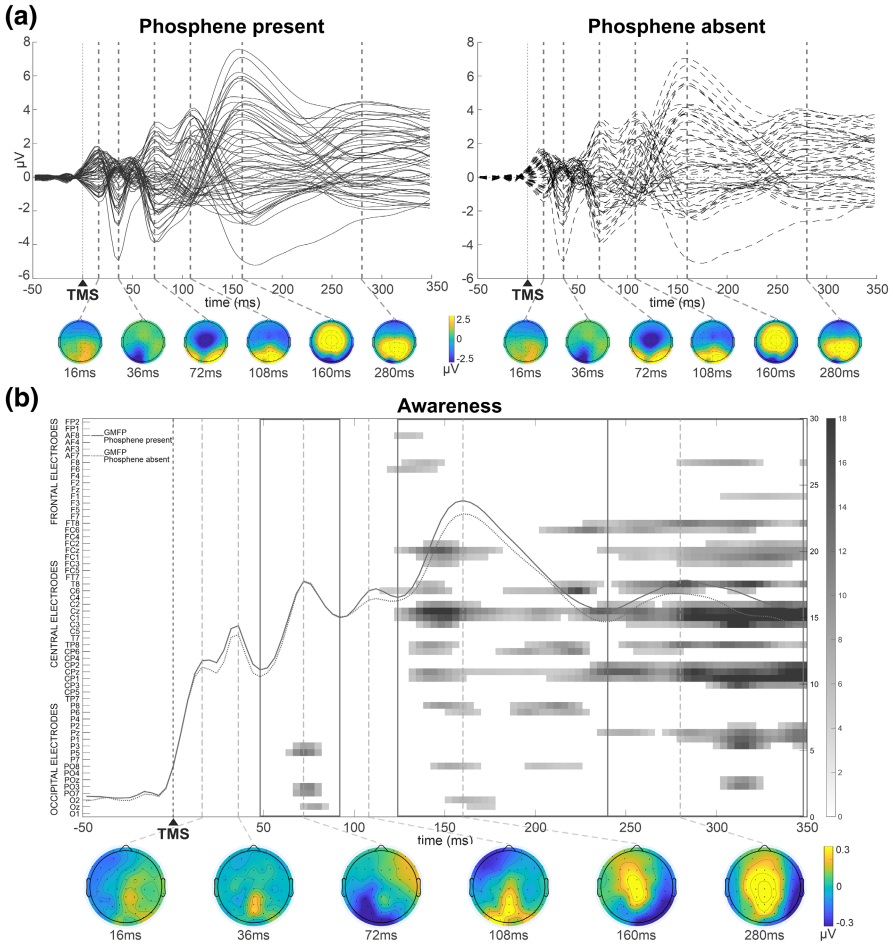

FIGURE 5 Results from the ANOVA conducted on TEPs: main effects of "phosphene awareness". (a) Butterfly plots depicting TEPs for the two *phosphene awareness* conditions ("phosphene present," continuous line; "phosphene absent," dotted line). Vertical dotted lines highlight the peaks of the different TEPs components. The scalp topographies below represent the scalp topographic distribution for each component peak. (b) Raster plot depicting for each time point and each electrode the significant differences (expressed in *F*-values) between "phosphene present" and "phosphene absent". Right TMS data were flipped so that stimulation sites were overlapped. *X* and *Y* axis represent, respectively, time in milliseconds and electrodes (from posterior to anterior ones). The two lines superimposed represent the GMFPs associated with the two *phosphene awareness* conditions, whose peaks were used to identify TEPs clusters. The vertical dotted lines highlight GMFPs peaks. The scalp topographies below represent scalp differences between the two conditions ("phosphene present"–"phosphene absent"), with each map corresponding to the latency of each GMFP peak.

right-hemispheric specialization with regard to visual processing. Moreover, we also found a significant difference in the RTs between perceived and not perceived phosphenes, with the former being significantly faster than the latter. This is an index of reliability of the participants' responses: it shows that phosphenes are reported at the end of a self-terminating search, which, in the case of negative responses, lasts longer due to the wait for a phosphene to appear.

Comparing the gISP index determined by right and left TMS in five temporal windows, we detected differences in how TMS-induced activity spreads across the electrodes during the time window ranging from 92 to 124 ms: after left TMS, activity tends to diffuse contralaterally more than after right stimulation, pointing toward the existence of connectivity differences following right and left early visual areas stimulation. This is also supported by our LMFP results, showing that left TMS elicits a higher activity in the contralateral hemisphere, compared to right TMS: this pinpoints to a hemispheric transfer of signal after left TMS which is not present after right TMS, suggesting the existence of hemispheric differences in how signal originating from early visual areas spreads across the brain.

With regard to phosphenes perception, TEP analysis showed the existence of hemispheric differences between the two early visual cortices. Phosphenes after left TMS are associated with early occipito-parietal and frontal activity, while at later latencies central electrodes are progressively more involved; phosphenes after right TMS determine

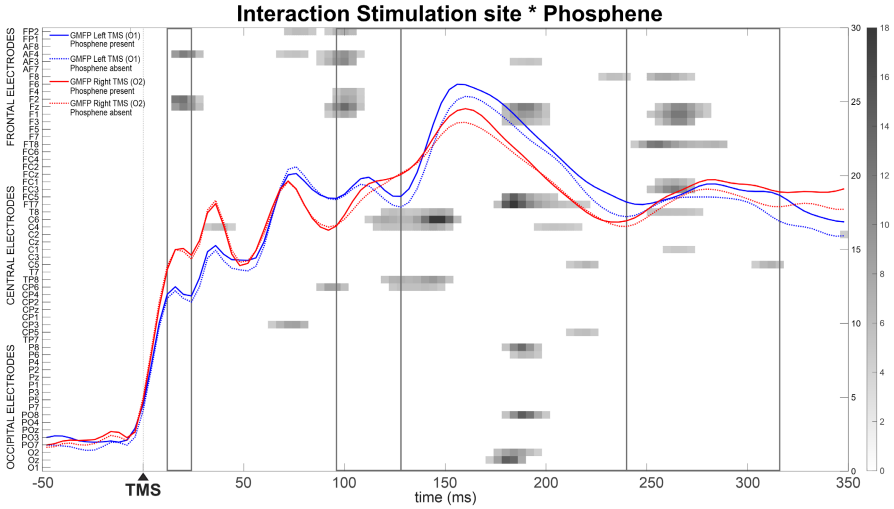

FIGURE 6 Results from the ANOVA conducted on TEPs: interaction between "stimulation site" and "phosphene awareness." Raster plot depicting for each time point and each electrode the significant differences (expressed in *F*-values) between the four different conditions ("Left TMS-Phosphene present"; "Left TMS-Phosphene absent"; "Right TMS-Phosphene present"; "Right TMS-Phosphene absent"). *X* and *Y* axis, respectively, represent time in milliseconds and electrodes (from posterior to anterior ones). The four lines superimposed represent the GMFPs associated with the four conditions, whose peaks were used to identify TEPs clusters.

only late and central activations, with a marginal contribution of parietal and frontal areas.

Over the last years, only a handful of studies have started reporting hemispheric differences after administering TMS to early occipital areas. Among these, Garcia et al. (2011) have stimulated with TMS various homologue visual areas in both hemispheres, including the early visual cortex. They reported hemispheric asymmetries in the magnitude and the responses following lateralized V1 stimulation, especially at 40 ms after the stimulation. This goes in the direction of our LMFP results, where we report a difference from 16 to 28 ms between the two stimulation sites; while being slightly earlier than that reported by Garcia and colleagues, our result suggests the existence of early differences in the electrophysiological response to TMS of early visual areas. This discrepancy between left and right V1/V2 also emerges with regard to phosphene perception: phosphenes elicited by right and left TMS are associated with distinctive brain responses, suggesting that these differences might not be simply due to different connectivity but might play a role in visual perception.

Jarczok et al. (2021), in another TMS-EEG study, focused on the interhemispheric differences in the brain response to lateralized TMS administration. Although in their analysis they did not specifically focus on the reported TEPs, it is nonetheless apparent the presence of hemispheric differences in TEPs topographies evoked by either right or left stimulation. Differences are maximally apparent between 80 and 100 ms over central and parieto-occipital electrodes, fading progressively as the epoch continues; this partially mirrors our TEP results, which show, in a similar time window, a difference over fronto-central electrodes as a function of the stimulation site. Despite the similarities, comparisons between our results and those from Jarczok and colleagues must be cautious: while our TMS locations were centered around electrodes O1 and O2, they stimulated between electrodes P7/P8 and P11/12, and this might account for the differences in TEPs topographies. Nevertheless, our results are in accordance with the presence of differences in a time window around 100 ms after left and right TMS stimulation of early visual areas.

Hemispheric differences in connectivity have also been investigated via TMS-fMRI. Ruff et al. (2009) analyzed how TMS over the right and left fronto-parietal cortex affected occipital activity in the two hemispheres. Effects of frontal and parietal stimulation were markedly different in the two hemispheres. Both left and right frontal TMS decreased the activity in central visual field representations, but only right frontal stimulation was able to increase activity in the peripheral field representations in the occipital lobe of both hemispheres. These differences were even more evident with parietal stimulation: only right parietal TMS was able to modulate activity in the visual cortex of both hemispheres. This hemispheric asymmetry may derive from the predominance of the right hemisphere in visual processing (Cavézian et al., 2015) and thus explains its major capability in influencing the signal in the occipital cortex bilaterally. This view is also supported by our LMFP and gISP results: we report a higher contralateral activity after left TMS compared to right around 100 ms after the stimulation, particularly localized over fronto-central electrodes. These imbalanced activations could reflect feedforward connections between left occipital

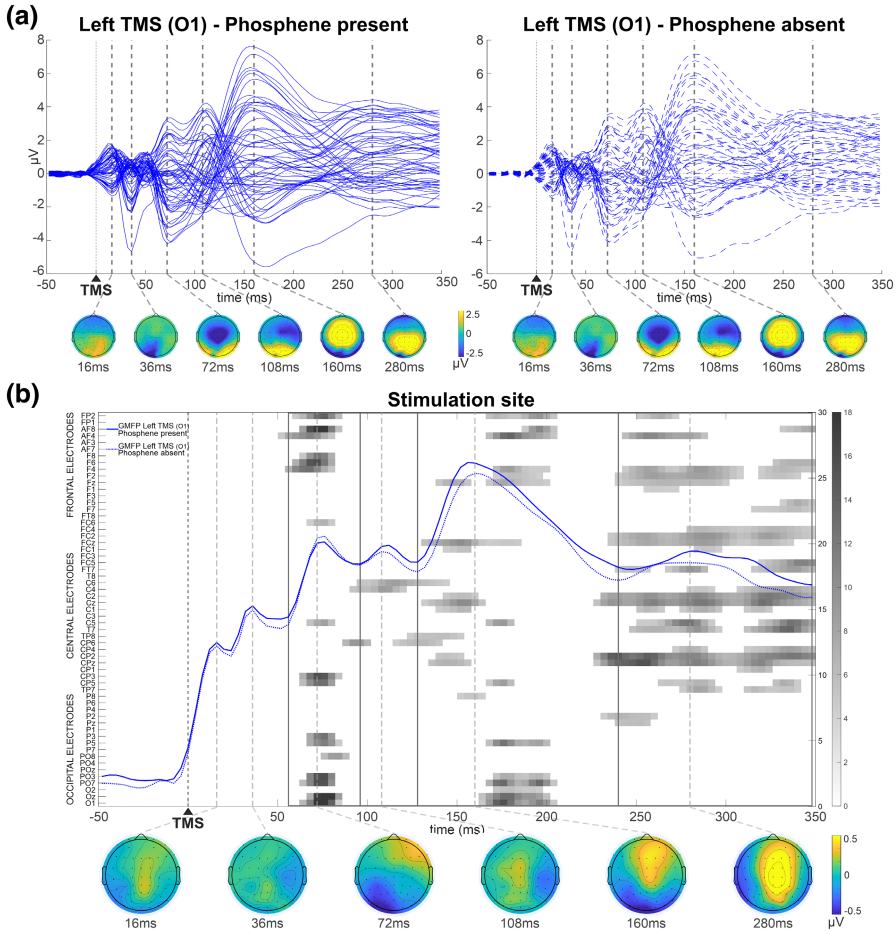

FIGURE 7 Results from the ANOVA conducted on TEPs: post hoc pairwise comparison between "Left TMS-Phosphene present" and "Left TMS-Phosphene absent". (a) Butterfly plots depicting TEPs for the two *Left TMS* conditions ("Left TMS-Phosphene present," blue continuous line; "Left TMS-Phosphene absent," blue dotted line). Vertical dotted lines highlight the peaks of the different TEPs components. The scalp topographies below represent the scalp topographic distribution for each component peak. (b) Raster plot depicting for each time point and each electrode the significant differences (expressed in *t*-values) between "Left TMS-Phosphene present" and "Left TMS-Phosphene absent." *X* and *Y* axis represent, respectively, time in milliseconds and electrodes (from posterior to anterior ones). The two lines superimposed represent the GMFPs associated with the two *Left TMS* conditions, whose peaks were used to identify TEPs clusters. The vertical dotted lines highlight GMFPs peaks. The scalp topographies below represent scalp differences between the two conditions ("Left TMS-Phosphene present"–"Left TMS-Phosphene absent"), with each map corresponding to the latency of each GMFP peak.

and right fronto-central areas, responsible for transferring visual stimuli to the competent hemisphere. While comparing these results, however, it is necessary to consider that they are obtained through different neuroimaging techniques and that while our results supposedly go in the direction of a bottom-up connection, Ruff and colleagues have investigated top-down projections, preventing us from drawing direct comparisons.

In a recent paper, Siviero et al. (2023) analyzed the same data sets through the use of effective connectivity and graph networks, confirming the reliability of our conclusions. Effective connectivity is characterized as the influence that one neural system has over another via causal or non-causal effects (Friston, 2011): it allows to understand how the different information flows are integrated within the brain network, clarifying specific pathways of neural activity. With respect to functional connectivity, effective connectivity allows to distinguish the direction of the flowing information. Graph theory, on the other side, is a powerful tool to represent brain connectivity, allowing to represent the brain as a network of interconnected nodes and links, representing respectively brain regions and relationships between those regions. Through the combination of effective connectivity and graph network, Siviero et al. found that left occipital stimulation activated mainly right channels contralateral to the stimulation, particularly those located over frontal areas. On the other side, right occipital stimulation determined increased intra-hemispheric connectivity, with right occipital and frontal electrodes ipsilateral to the stimulation increasing their connections. Results in this paper confirm our conclusions: in fact, while employing

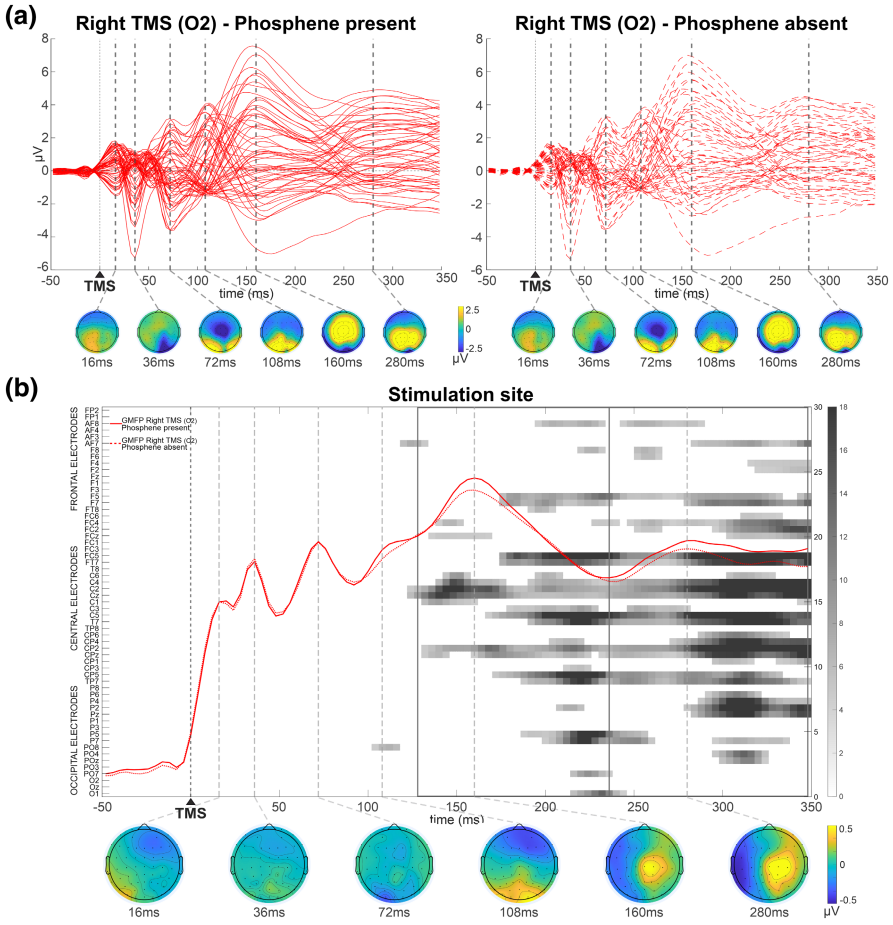

FIGURE 8 Results from the ANOVA conducted on TEPs: post hoc pairwise comparison between "O2-Phosphene present" and "O2-Phosphene absent." (a) Butterfly plots depicting TEPs for the two *Right TMS* conditions ("Right TMS-Phosphene present," red continuous line; "Right TMS-Phosphene absent," red dotted line). Vertical dotted lines highlight the peaks of the different TEPs components. The scalp topographies below represent the scalp topographic distribution for each component peak. (b) Raster plot depicting for each time point and each electrode the significant differences (expressed in *t*-values) between "Right TMS-Phosphene present" and "Right TMS-Phosphene absent." *X* and *Y* axis represent, respectively, time in milliseconds and electrodes (from posterior to anterior ones). The two lines superimposed represent the GMFPs associated with the two *Right TMS* conditions, whose peaks were used to identify TEPs clusters. The vertical dotted lines highlight GMFPs peaks. The scalp topographies below represent scalp differences between the two conditions ("Right TMS-Phosphene present"–"Right TMS-Phosphene absent"), with each map corresponding to the latency of each GMFP peak.

a different analytical approach, they still manage to show the existence of a hemispheric asymmetry between the two hemispheres, with the right hemisphere being activated by both left and right occipital stimulation. Occipital stimulation determined side-specific spatio-temporal dynamics, providing further support to our claim for a right-hemispheric specialization for handling visual information.

Another critical point deserving consideration relates to the electrophysiological correlates of phosphene perception: to the best of our knowledge, ours is the first study that systematically explored them across the two hemispheres in the healthy brain (Mazzi, Mazzeo, et al., 2017). Bagattini et al. (2015) recorded EEG activity associated with phosphene perception after left occipital TMS stimulation. Their results show the presence of bilateral differential activity over centro-temporal electrodes in a time window from 70 to 90 ms, followed by a late occipital activation starting around 320 ms until the end of the epoch. Our earliest differential activity is present from 50 to 90 ms over frontal and parieto-occipital electrodes, followed by later more spread activity including frontal, central, and parieto-occipital electrodes. Bagattini and colleagues' results are in partial accordance with what we detected here: for example, both the studies suggest the existence of an early critical time window for phosphene perception after left occipital TMS, occurring between 50 and 100 ms. Discrepancies in results might be due to differences in the EEG analysis pipeline and to the absence of individual MRI images in the study by Bagattini et al., which might have prevented in some participants the proper

targeting of early visual areas. TMS differential activity after right occipital TMS stimulation has been reported by Taylor et al. (2010). They describe two late activations spread over centro-parietal electrodes: the first between 160 and 200 ms, and the second between 280 and 400 ms. These results closely match those from our study: our first cluster of differential activity begins at 130 and ends at 240 ms, followed by a second one starting at 240 ms up until 320 ms; both are based on a bilaterally widespread centro-parietal activation. Similarly to Taylor et al., we relate phosphenes perception after right TMS to late, central electrophysiological activity.

Taken together, our results suggest the existence of different spatio-temporal dynamics resulting from the stimulation of the early visual cortices of the two hemispheres with regard to phosphene perception. On the one side, left occipital stimulation elicits earlier activity, initially limited to occipito-parietal and frontal electrodes, which gradually spreads toward fronto-central locations; on the other side, right occipital stimulation bypasses any early posterior activation, activating a late bilateral central cluster that lasts basically unaltered for the duration of the entire epoch. This difference may again be related to the predominance of the right hemisphere compared to the left one in visual processing—as also suggested by faster RTs following right occipital stimulation: while early activations in the right hemisphere are so strong that differences between the two phosphenes conditions (present/absent) cannot properly emerge (suggesting a "rooftop effect," also supported by our LMFP data showing higher early activity after O2 stimulation), stimulation of the left hemisphere, eliciting weaker activity, allows to disentangle phosphenes conditions from an earlier time point.

As pointed out above, different lateralized brain areas have been listed as responsible for processing different aspects of visual stimuli (Kauffmann et al., 2014); however, the electrophysiological mechanisms sustaining these different processes are still largely unknown. Although not specifically addressed in this study, the differences we detected after lateralized occipital stimulation might represent activity patterns responsible for the functional differentiation of the two hemispheres.

It is now known that early TEPs components reflect aspects of local excitability in the stimulated area, while later TEPs components are related to trans-synaptical connectivity, mainly regulated by GABAergic inhibitory neurons (Casula et al., 2018; Premoli et al., 2014; Rogasch et al., 2013). Our results seem to hint at the possibility of a hemispheric asymmetry in these mechanisms following occipital stimulation, with activity originating from the left hemisphere spreading more easily to the contralateral hemisphere than activity from the right hemisphere. A further investigation on the possible existence of this kind of hemispheric asymmetries is warranted.

Characterizing the electrophysiological activity giving rise to visual perception is a step of fundamental importance in the context of reestabilishing visual capacities in patients affected by forms of cortical blindness. Patients suffering from occipital infarction can incur in a number of changes in vision, such as hemianopia, which can heavily impact daily functions, reducing personal autonomy and overall diminishing quality of life (Brandt et al., 2000; Tharaldsen et al., 2020). It is of primary importance, therefore, to establish a "ground truth" when it comes to the description of the electrophysiological processes sustaining conscious vision: in this way, the reestablishing of such processes in case of brain injury could constitute a clinical and pharmacological target able to restore—at least partly—visual capacities in brain-injured patients. It is now known, in fact, that EEG activity is consistently imbalanced in stroke patients, and that a restoration of its more usual values can predict stroke recovery (Lanzone et al., 2022). For this to be possible also for occipitally injured patients, however, it is necessary to find the electrophysiological characteristics of a healthy visual system.

In conclusion, our study shows that the brain response after early visual cortex stimulation differs between right and left hemispheres and that the activations associated with phosphene perception present a different pattern in the two hemispheres. Future studies will investigate the possible presence of these asymmetric activations also in other phosphene sites (Bagattini et al., 2015; Guzman-Lopez et al., 2011; Mazzi, Mazzeo, et al., 2017).

AUTHOR CONTRIBUTIONS

Davide Bonfanti: Formal analysis; investigation; software; visualization; writing – original draft. **Chiara Mazzi:** Conceptualization; formal analysis; investigation; methodology; software; supervision; visualization; writing – review and editing. **Silvia Savazzi:** Conceptualization; software; funding acquisition; methodology; supervision; writing – review and editing.

FUNDING INFORMATION

This research was supported by #NEXTGENERATIONEU (NGEU) and funded by the Ministry of University and Research (MUR), National Recovery and Resilience Plan (NRRP), project MNESYS (PE0000006)—A Multiscale integrated approach to the study of the nervous system in health and disease (DN. 1553 11.10.2022), MIUR PRIN 2017 (grant no. 2017TBA4KS_002) and by Fondazione Cassa di Risparmio di Verona Vicenza Belluno e Ancona "Ricerca scientifica d'eccellenza 2018"

(grant no. 2018.0861). C.M. was supported by MIUR D.M. 737/2021—"Neural correlates of perceptual awareness: from neural architecture to the preservation of conscious vision in brain tumor patients".

CONFLICT OF INTEREST STATEMENT

None.

DATA AVAILABILITY STATEMENT

The data supporting the conclusions of this article are publicly available at: https://gin.g-node.org/DB_123/Phosphenes_occipital.

ORCID

Davide Bonfanti https://orcid.org/0000-0001-7858-8244
Chiara Mazzi https://orcid.org/0000-0002-4966-9341

REFERENCES

Bagattini, C., Mazzi, C., & Savazzi, S. (2015). Waves of awareness for occipital and parietal phosphenes perception. *Neuropsychologia*, *70*, 114–125. https://doi.org/10.1016/j.neuropsychologia.2015.02.021

Ben-Shachar, M. S. (2020). *TBT: Reject and interpolate channels on a epoch by epoch basis (2.6.1)*. Zenodo. https://doi.org/10.5281/ZENODO.3784278

Brandt, T., Steinke, W., Thie, A., Pessin, M. S., & Caplan, L. R. (2000). Posterior cerebral artery territory infarcts: Clinical features, infarct topography, causes and outcome. Multicenter results and a review of the literature. *Cerebrovascular Diseases*, *10*(3), 170–182. https://doi.org/10.1159/000016053

Casula, E. P., Maiella, M., Pellicciari, M. C., Porrazzini, F., D'Acunto, A., Rocchi, L., & Koch, G. (2020). Novel TMS-EEG indexes to investigate interhemispheric dynamics in humans. *Clinical Neurophysiology*, *131*(1), 70–77. https://doi.org/10.1016/j.clinph.2019.09.013

Casula, E. P., Mayer, I. M. S., Desikan, M., Tabrizi, S. J., Rothwell, J. C., & Orth, M. (2018). Motor cortex synchronization influences the rhythm of motor performance in premanifest huntington's disease. *Movement Disorders*, *33*(3), 440–448. https://doi.org/10.1002/MDS.27285

Cavézian, C., Perez, C., Peyrin, C., Gaudry, I., Obadia, M., Gout, O., & Chokron, S. (2015). Hemisphere-dependent ipsilesional deficits in hemianopia: Sightblindness in the "intact" visual field. *Cortex*, *69*, 166–174. https://doi.org/10.1016/j.cortex.2015.05.010

Chokron, S., Perez, C., & Peyrin, C. (2016). Behavioral consequences and cortical reorganization in homonymous hemianopia. *Frontiers in Systems Neuroscience*, *10*, 57. https://doi.org/10.3389/fnsys.2016.00057

Delorme, A., & Makeig, S. (2004). EEGLAB: An open source toolbox for analysis of single-trial EEG dynamics including independent component analysis. *Journal of Neuroscience Methods*, *134*, 9–21. https://doi.org/10.1016/j.jneumeth.2003.10.009

Delorme, A., Sejnowski, T., & Makeig, S. (2007). Enhanced detection of artifacts in EEG data using higher-order statistics and independent component analysis. *NeuroImage*, *34*(4), 1443–1449. https://doi.org/10.1016/J.NEUROIMAGE.2006.11.004

Dong, L., Li, F., Liu, Q., Wen, X., Lai, Y., Xu, P., & Yao, D. (2017). MATLAB toolboxes for reference electrode standardization technique (REST) of scalp EEG. *Frontiers in Neuroscience*, *11*, 601. https://doi.org/10.3389/fnins.2017.00601

Fink, G. R., Halligan, P. W., Marshall, J. C., Frith, C. D., Frackowiak, R. S. J., & Dolan, R. J. (1996). Where in the brain does visual attention select the forest and the trees? *Nature*, *382*(6592), 626–629. https://doi.org/10.1038/382626a0

Fink, G. R., Halligan, P. W., Marshall, J. C., Frith, C. D., Frackowiak, R. S. J., Dolan, R. J., & Neurology, W. (1997). Neural mechanisms involved in the processing of global and local aspects of hierarchically organized visual stimuli. *Brain*, *120*, 1779–1791.

Friston, K. J. (2011). Functional and effective connectivity: A review. *Brain Connectivity*, *1*(1), 13–36. https://doi.org/10.1089/BRAIN.2011.0008

Garcia, J. O., Grossman, E. D., & Srinivasan, R. (2011). Evoked potentials in large-scale cortical networks elicited by TMS of the visual cortex. *Journal of Neurophysiology*, *106*, 1734–1746. https://doi.org/10.1152/jn.00739.2010.-Single

Groppe, D. M., Urbach, T. P., & Kutas, M. (2011). Mass univariate analysis of event-related brain potentials/fields I: A critical tutorial review. *Psychophysiology*, *48*(12), 1711–1725. https://doi.org/10.1111/J.1469-8986.2011.01273.X

Guzman-Lopez, J., Silvanto, J., Yousif, N., Nousi, S., Quadir, S., & Seemungal, B. M. (2011). Probing V5/MT excitability with transcranial magnetic stimulation following visual motion adaptation to random and coherent motion. *Annals of the New York Academy of Sciences*, *1233*(1), 200–207. https://doi.org/10.1111/J.1749-6632.2011.06179.X

Hellige, J. B. (1996). Hemispheric asymmetry for visual information processing. *Acta Neurobiologiae Experimentalis*, *56*(1), 485–497.

Hui, J., Zomorrodi, R., Lioumis, P., Ensafi, E., Voineskos, D., Voineskos, A., Hadas, I., Rajji, T. K., Blumberger, D. M., & Daskalakis, Z. J. (2021). Altered interhemispheric signal propagation in schizophrenia and depression. *Clinical Neurophysiology*, *132*(7), 1604–1611. https://doi.org/10.1016/j.clinph.2021.03.039

Jarczok, T. A., Fritsch, M., Kröger, A., Schneider, A. L., Althen, H., Siniatchkin, M., Freitag, C. M., & Bender, S. (2016). Maturation of interhemispheric signal propagation in autism spectrum disorder and typically developing controls: A TMS-EEG study. *Journal of Neural Transmission*, *123*(8), 925–935. https://doi.org/10.1007/s00702-016-1550-5

Jarczok, T. A., Roebruck, F., Pokorny, L., Biermann, L., Roessner, V., Klein, C., & Bender, S. (2021). Single-pulse TMS to the temporo-occipital and dorsolateral prefrontal cortex evokes lateralized long latency EEG responses at the stimulation site. *Frontiers in Neuroscience*, *15*, 616667. https://doi.org/10.3389/fnins.2021.616667

JASP Team. (2020). *JASP* (0.13.1).

Kammer, T., Puls, K., Erb, M., & Grodd, W. (2005). Transcranial magnetic stimulation in the visual system. II. Characterization of induced phosphenes and scotomas. *Experimental Brain Research*, *160*(1), 129–140. https://doi.org/10.1007/s00221-004-1992-0

Kauffmann, L., Ramanoël, S., & Peyrin, C. (2014). The neural bases of spatial frequency processing during scene perception. *Frontiers in Integrative Neuroscience*, *8*, 37. https://doi.org/10.3389/fnint.2014.00037

Kitterle, F. L., Christman, S., & Hellige, J. B. (1990). Hemispheric differences are found in the identification, but not the detection, of

low versus high spatial frequencies. *Perception & Psychophysics*, *48*(4), 297–306.

Knight, R., Mazzi, C., & Savazzi, S. (2015a). Assessing the effects of physical and perceived luminance contrast on RT and TMS-induced percepts. *Experimental Brain Research*, *233*, 3527–3534. https://doi.org/10.1007/s00221-015-4419-1

Knight, R., Mazzi, C., & Savazzi, S. (2015b). Shining new light on dark percepts: Visual sensations induced by TMS. *Experimental Brain Research*, *233*(11), 3125–3132. https://doi.org/10.1007/S00221-015-4381-Y

Lanzone, J., Colombo, M. A., Sarasso, S., Zappasodi, F., Rosanova, M., Massimini, M., Di Lazzaro, V., & Assenza, G. (2022). EEG spectral exponent as a synthetic index for the longitudinal assessment of stroke recovery. *Clinical Neurophysiology*, *137*, 92–101. https://doi.org/10.1016/j.clinph.2022.02.022

Lehmann, D., & Skrandies, W. (1980). Reference-free identification of components of checkerboard-evoked multichannel potential fields. *Electroencephalography and Clinical Neurophysiology*, *48*(6), 609–621. https://doi.org/10.1016/0013-4694(80)90419-8

Lux, S., Marshall, J. C., Ritzl, A., Weiss, P. H., Pietrzyk, U., Shah, N. J., Zilles, K., & Fink, G. R. (2004). A functional magnetic resonance imaging study of local/global processing with stimulus presentation in the peripheral visual hemifields. *Neuroscience*, *124*(1), 113–120. https://doi.org/10.1016/j.neuroscience.2003.10.044

Marzi, C. A., Bisiacchi, P., & Nicoletti, R. (1991). Is interhemispheric transfer of visuomotor information asymmetric? Evidence from a meta-analysis. *Neuropsychologia*, *29*(12), 1163–1177. https://doi.org/10.1016/0028-3932(91)90031-3

Mazzi, C., Mancini, F., & Savazzi, S. (2014). Can IPS reach visual awareness without V1? Evidence from TMS in healthy subjects and hemianopic patients. *Neuropsychologia*, *64*, 134–144. https://doi.org/10.1016/j.neuropsychologia.2014.09.026

Mazzi, C., Mazzeo, G., & Savazzi, S. (2017). Markers of TMS-evoked visual conscious experience in a patient with altitudinal hemianopia. *Consciousness and Cognition*, *54*, 143–154. https://doi.org/10.1016/j.concog.2017.01.022

Mazzi, C., Savazzi, S., Abrahamyan, A., & Ruzzoli, M. (2017). Reliability of TMS phosphene threshold estimation: Toward a standardized protocol. *Brain Stimulation*, *10*(3), 609–617. https://doi.org/10.1016/j.brs.2017.01.582

Meikle, S. J., & Wong, Y. T. (2022). Neurophysiological considerations for visual implants. *Brain Structure & Function*, *227*(4), 1523–1543. https://doi.org/10.1007/S00429-021-02417-2

Musel, B., Bordier, C., Dojat, M., Pichat, C., Chokron, S., Le Bas, J. F., & Peyrin, C. (2013). Retinotopic and lateralized processing of spatial frequencies in human visual cortex during scene categorization. *Journal of Cognitive Neuroscience*, *25*(8), 1315–1331. https://doi.org/10.1162/jocn_a_00397

Oldfield, R. C. (1971). The assessment and analysis of handedness: The Edinburgh inventory. *Neuropsychologia*, *9*(1), 97–113. https://doi.org/10.1016/0028-3932(71)90067-4

Pernet, C. R., Chauveau, N., Gaspar, C., & Rousselet, G. A. (2011). LIMO EEG: A toolbox for hierarchical LInear MOdeling of ElectroEncephaloGraphic data. *Computational Intelligence and Neuroscience*, *2011*, 1–11. https://doi.org/10.1155/2011/831409

Peyrin, C., Baciu, M., Segebarth, C., & Marendaz, C. (2004). Cerebral regions and hemispheric specialization for processing spatial frequencies during natural scene recognition. An event-related fMRI study. *NeuroImage*, *23*(2), 698–707. https://doi.org/10.1016/j.neuroimage.2004.06.020

Peyrin, C., Chauvin, A., Chokron, S., & Marendaz, C. (2003). Hemispheric specialization for spatial frequency processing in the analysis of natural scenes. *Brain and Cognition*, *53*(2), 278–282. https://doi.org/10.1016/S0278-2626(03)00126-X

Peyrin, C., Chokron, S., Guyader, N., Gout, O., Moret, J., & Marendaz, C. (2006). Neural correlates of spatial frequency processing: A neuropsychological approach. *Brain Research*, *1073–1074*(1), 1–10. https://doi.org/10.1016/j.brainres.2005.12.051

Peyrin, C., Schwartz, S., Seghier, M., Michel, C., Landis, T., & Vuilleumier, P. (2005). Hemispheric specialization of human inferior temporal cortex during coarse-to-fine and fine-to-coarse analysis of natural visual scenes. *NeuroImage*, *28*(2), 464–473. https://doi.org/10.1016/j.neuroimage.2005.06.006

Premoli, I., Castellanos, N., Rivolta, D., Belardinelli, P., Bajo, R., Zipser, C., Espenhahn, S., Heidegger, T., Müller-Dahlhaus, F., & Ziemann, U. (2014). TMS-EEG signatures of GABAergic neurotransmission in the human cortex. *Journal of Neuroscience*, *34*, 5603–5612. https://doi.org/10.1523/JNEUROSCI.5089-13.2014

Proverbio, A. M., Zani, A., & Avella, C. (1996). Differential activation of multiple current sources of foveal VEPs as a function of spatial frequency. *Brain Topography*, *9*(1), 59–68. https://doi.org/10.1007/BF01191643

Robertson, L. C., Lamb, M. R., & Knight, R. T. (1988). Effects of lesions of temporal-parietal junction on perceptual and attentional processing in humans. *Journal of Neuroscience*, *8*(10), 3757–3769. https://doi.org/10.1523/jneurosci.08-10-03757.1988

Rogasch, N. C., Daskalakis, Z. J., & Fitzgerald, P. B. (2013). Mechanisms underlying long-interval cortical inhibition in the human motor cortex: A TMS-EEG study. *Journal of Neurophysiology*, *109*(1), 89–98. https://doi.org/10.1152/JN.00762.2012

Rogasch, N. C., Sullivan, C., Thomson, R. H., Rose, N. S., Bailey, N. W., Fitzgerald, P. B., Farzan, F., & Hernandez-Pavon, J. C. (2017). Analysing concurrent transcranial magnetic stimulation and electroencephalographic data: A review and introduction to the open-source TESA software. *NeuroImage*, *147*, 934–951. https://doi.org/10.1016/j.neuroimage.2016.10.031

Rosanova, M., Casarotto, S., Pigorini, A., Canali, P., Casali, A. G., & Massimini, M. (2012). Combining transcranial magnetic stimulation with electroencephalography to study human cortical excitability and effective connectivity. *NeuroMethods*, *67*, 435–457. https://doi.org/10.1007/7657_2011_15

Rossi, S., Hallett, M., Rossini, P. M., Pascual-Leone, A., Avanzini, G., Bestmann, S., Berardelli, A., Brewer, C., Canli, T., Cantello, R., Chen, R., Classen, J., Demitrack, M., Di Lazzaro, V., Epstein, C. M., George, M. S., Fregni, F., Ilmoniemi, R., Jalinous, R., ... Ziemann, U. (2009). Safety, ethical considerations, and application guidelines for the use of transcranial magnetic stimulation in clinical practice and research. *Clinical Neurophysiology*, *120*(12), 2008–2039. https://doi.org/10.1016/j.clinph.2009.08.016

Ruff, C. C., Blankenburg, F., Bjoertomt, O., Bestmann, S., Weiskopf, N., & Driver, J. (2009). Hemispheric differences in frontal and parietal influences on human occipital cortex: Direct confirmation with concurrent TMS–fMRI. *Journal of Cognitive Neuroscience*, *21*(6), 1146–1161. https://doi.org/10.1162/JOCN.2009.21097

Sanchez-Lopez, J., Savazzi, S., Pedersini, C. A., Cardobi, N., & Marzi, C. A. (2020). Neural bases of unconscious orienting of attention in hemianopic patients: Hemispheric differences. *Cortex*, *127*, 269–289. https://doi.org/10.1016/j.cortex.2020.02.015

Sergent, J. (1982). The cerebral balance of power: Confrontation or cooperation? *Journal of Experimental Psychology: Human Perception and Performance*, *8*(2), 253–272. https://doi.org/10.1037/0096-1523.8.2.253

Siviero, I., Bonfanti, D., Menegaz, G., Savazzi, S., Mazzi, C., & Storti, S. F. (2023). Graph analysis of TMS–EEG connectivity reveals hemispheric differences following occipital stimulation. *Sensors*, *23*(21), 8833. https://doi.org/10.3390/s23218833

Taylor, P. C. J., Walsh, V., & Eimer, M. (2010). The neural signature of phosphene perception. *Human Brain Mapping*, *31*(9), 1408–1417. https://doi.org/10.1002/hbm.20941

Tharaldsen, A. R., Sand, K. M., Dalen, I., Wilhelmsen, G., Næss, H., Midelfart, A., Rødahl, E., Thomassen, L., Hoff, J. M., Frid, L. M., Tandstad, H. K., Hegreberg, G., Lundberg, K., Karlsen, T. R., Setseng, B., Rohweder, G., Indredavik, B., Kurz, M. W., & Idicula, T. (2020). Vision-related quality of life in patients with occipital stroke. *Acta Neurologica Scandinavica*, *141*(6), 509–518. https://doi.org/10.1111/ANE.13232

Voineskos, A. N., Farzan, F., Barr, M. S., Lobaugh, N. J., Mulsant, B. H., Chen, R., Fitzgerald, P. B., & Daskalakis, Z. J. (2010). The role of the corpus callosum in transcranial magnetic stimulation induced interhemispheric signal propagation. *Biological Psychiatry*, *68*(9), 825–831. https://doi.org/10.1016/j.biopsych.2010.06.021

Yao, D. (2001). A method to standardize a reference of scalp EEG recordings to a point at infinity. *Physiological Measurement*, *22*(4), 693–711. https://doi.org/10.1088/0967-3334/22/4/305

How to cite this article: Bonfanti, D., Mazzi, C., & Savazzi, S. (2024). Mapping the routes of perception: Hemispheric asymmetries in signal propagation dynamics. *Psychophysiology*, *00*, e14529. https://doi.org/10.1111/psyp.14529